Organic & Biomolecular Chemistry

Accepted Manuscript

This is an *Accepted Manuscript*, which has been through the Royal Society of Chemistry peer review process and has been accepted for publication.

Accepted Manuscripts are published online shortly after acceptance, before technical editing, formatting and proof reading. Using this free service, authors can make their results available to the community, in citable form, before we publish the edited article. We will replace this *Accepted Manuscript* with the edited and formatted *Advance Article* as soon as it is available.

You can find more information about *Accepted Manuscripts* in the Information for Authors.

Please note that technical editing may introduce minor changes to the text and/or graphics, which may alter content. The journal's standard Terms & Conditions and the Ethical guidelines still apply. In no event shall the Royal Society of Chemistry be held responsible for any errors or omissions in this *Accepted Manuscript* or any consequences arising from the use of any information it contains.

ROYAL SOCIETY OF CHEMISTRY

www.rsc.org/obc

Journal Name
Organic & Biomolecular Chemistry
Dynamic Article Links ►

Cite this: DOI: 10.1039/c0xx00000x

www.rsc.org/xxxxxx

ARTICLE TYPE

On the Dynamics, Energetics and Selectivity of Water Chain-Containing Aquapores Created by the Self-Assembly of Aquafoldamer Molecules

Wenliang Ma,[a] Chunquan Wang,[a] Juntong Li,[a] Kun Zhang,[a,b] Yu-Jing Lu,*[a] Yanping Huo,*[a] and Huaqiang Zeng*[,c]

Received (in XXX, XXX) Xth XXXXXXXXX 20XX, Accepted Xth XXXXXXXXX 20XX
DOI: 10.1039/b000000x

Through a series of crystallographic snapshots of water chain-containing aquapores formed from numerous one-dimensionally aligned aquafoldamer molecules 2, we demonstrated here (1) a preferential recognition of the water molecules over methanol molecules by the assembled cavity-containing aquapores with a selectivity factor of at least 17.7, (2) a dynamic nature of the water chains and the aquapores in response to varying external stimuli that exert the most influential impact on the aromatic π-π stacking in the aquapores and (3) the aquapores undergo a significant re-arrangement in order to accommodate water, rather than methanol, molecules.

Introduction

Inspired by aquaporins' ability to trap one-dimensionally arrayed H-bonded water chains in their narrow channels and to selectively transport water molecules,[1] we have been interested in using supramolecular approach to mimic aquaporins in both structure and function with an ultimate aim to realize synthetic water channels for rapid and selective transport of water molecules for water purification. Such investigations are also in line with the recently emerged efforts,[2] focusing on creation of organic molecule-based hydrophilic[3] or hydrophobic[4] pores that are capable of hosting H-bonded 1D water chains and transporting water molecules[3f,5] and protons[3f,5a,6] across the bilayer membrane.

Our molecular strategy toward water recognition and transport builds upon our lasting interests in designing functional foldamer molecules[7] that are derived from methoxy,[8a-c] pyridone[8d, 8e] and fluorobenzene[8f,8g] build blocks. These folding molecules not only are able to adopt stable, compact conformations, but also perform many interesting functions including selective recognition of both ionic[8e,9a,9b] and neutral[9c,9d] species, solvent gelation,[8g] reaction sieving[9e,9f] and catalysis.[9g] By integrating computational modeling and crystallographic scrutiny, we recently envisioned and demonstrated the ability of intramolecular H-bonding forces to guide the folding of pyridine-based foldamer molecules such as pentamers **1** and **2** (Fig. 1) into a crescent or helically folded structure to enclose a cavity of ~ 2.8 Å in diameter defined by the interior amide protons.[10a] This small cavity rich in H-bond donors and acceptors matches well with the molecular dimensionality of water molecules measuring ~ 2.8 Å in diameter. Accordingly, short oligomers such as a trimer with a roughly planar geometry can bind one water molecule in their 2D planar cavity, while helically folded longer oligomers allow a water dimer to comfortably stay in their 3D-shaped helical cavity.[10b,10c] Terms of "aquafoldamer" and "aquapore" were then coined by us to describe these water-binding foldamer molecules and the pores contained within them.

Our recent continued exploration revealed that, by incorporating two electrostatically complementary functional groups into the two helical ends of helically folded aquapentamer **1**, the resultant helices possessing "sticky" ends (e.g., the ester and Cbz ends) could efficiently pile up via aromatic π-π stacking forces to produce one-dimensionally aligned helical stacks. This 1D packing further results in a hollow tubular cavity for inclusion of guest molecules such as methanol[11a] and dichloromethane.[11b] Through further subtle structural variations, a more rigid pyridine-based pentamer **2** was eventually discovered to produce similar 1D stacks containing well-aligned H-bonded 1D water chains in the formed narrow aquapores of ~ 2.8 Å in diameter. Functionally, these 1D water chains selectively transport water molecules across the bilayer membranes of large unilamellar vesicles of ~ 250 nm in diameter.[11c]

In the current work, we aim to provide additional insights into the functional hollow ensembles formed by **2** (e.g., the trapped water chains and self-assembled water-binding aquapores) in terms of dynamics, energetics, and selectivity by comparing crystallographic snapshots of the system in response to varying external stimuli and by computational calculations either at the B3LYP/6-311+G(2d,p) level or using Dreiding force field.[12a]

Results and discussion

Our early studies show that (1) slow diffusion of methanol into **1**-containing dichloromethane (CH_2Cl_2) solution gives rise to crystals **1**•MeOH containing regularly arrayed chains of methanol molecules in the hollow tubular cavity of $(\mathbf{1})_n$[11a] and (2) slow diffusion of acetone or ethyl acetate into **1**-containing CH_2Cl_2 produces crystals with CH_2Cl_2 molecules residing in the hollow cavity.[11b] Very surprisingly, even after re-growing or soaking the crystals of **1** in water-containing solvents, all the structural determinations of crystals reveal that only 24~40% of

Organic & Biomolecular Chemistry Accepted Manuscript

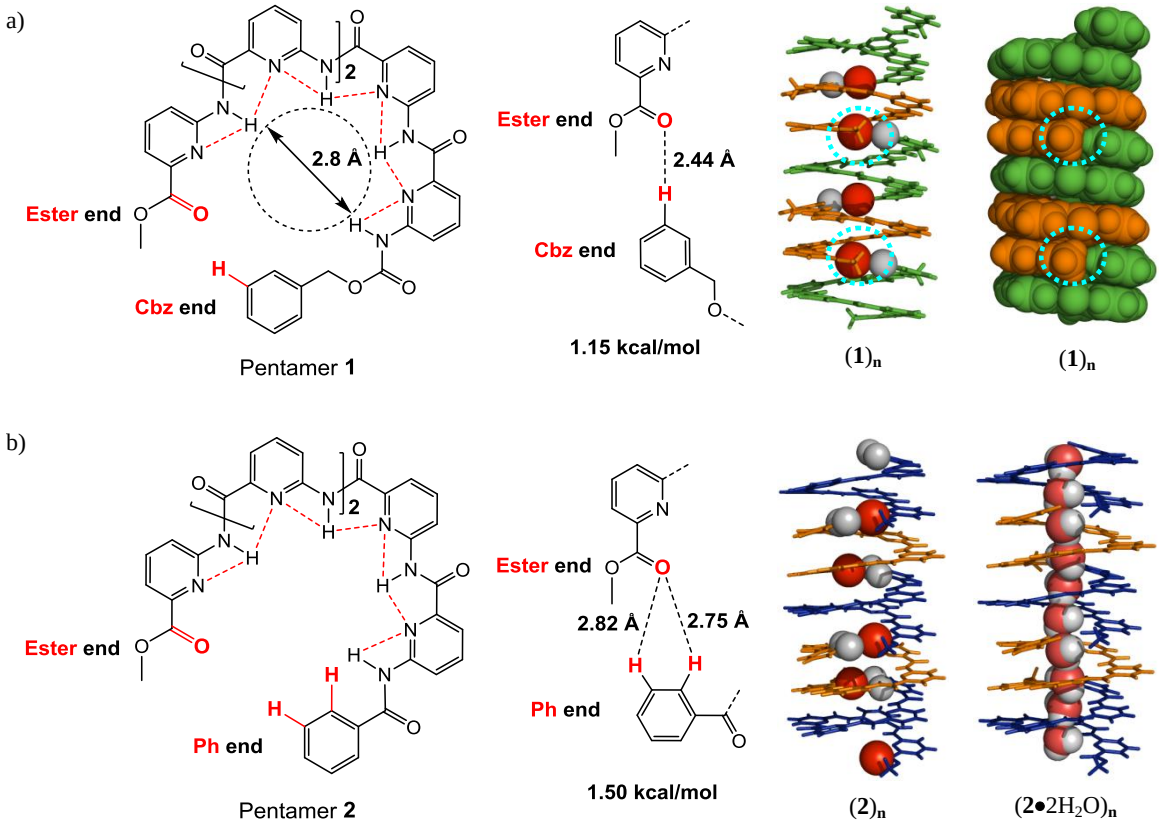

Fig. 1 (a) and (b) illustrate structures of pentamers **1** and **2**, respectively, which contain an interior cavity of ~ 2.8 Å in diameter defined by the interior amide protons, two "sticky" end groups (ester and Cbz or Ph groups) that are complementary to each other by virtue of a partially charged O-atom (H-bond acceptor) and an aromatic proton (H-bond donor) able to form weak intermolecular H-bonds of 2.44 Å, 2.75 Å and 2.82 Å with bond strengths of 1.15 and 1.50 kcal/mol computationally determined at the B3LYP/6-311G(2d,p) level, 1D chiral packing involving numerous molecules of **1** or **2** via complementary "sticky" end groups and aromatic π-π stacking forces. From CPK model of $(\mathbf{1})_n$ shown in (a), the 1D chiral stack appears to be built from a single chiral polymeric backbone, rather than from a copious amount of short oligomers. Also shown in (b) is the well-aligned 1D water chain trapped inside 1D chiral stack of $(\mathbf{2})_n$.

the MeOH molecules inside the interior of $(\mathbf{1})_n$ were replaced by water molecules, suggesting the recognition of H_2O molecules is preferred over CH_2Cl_2 molecules by the hollow cavity in $(\mathbf{1})_n$. A partial replacement of 24~40% of the MeOH molecules by H_2O is also in sharp contrast with the fact that other pentamers, differing from **1** by the two end groups, can readily accommodate two water molecules in their cavity even when the crystals were grown from anhydrous CH_2Cl_2.[10b,10c] These data suggest that the recognition of MeOH molecules by the hollow cavity in $(\mathbf{1})_n$ takes place in a selective manner with its binding affinity toward small guest molecules decreasing in the order of MeOH > H_2O > CH_2Cl_2 and that the hollow cavity in $(\mathbf{1})_n$ does not recognize other larger guests including acetone and ethyl acetate.

More surprisingly, we recently found that a small subtle structural modification, which involves a replacement of the more flexible Cbz group in **1** with a rigid phenyl ring as in **2**, renders molecules of **2** with an ability not only to form the desired 1D helical stacks mediated via two H-bonds between the two "sticky" ends but also to host H-bonded 1D water chains (see $(\mathbf{2}\bullet 2H_2O)_n$ in Fig. 1b).[11c] Similar to **1**, the 1D helical stacks made of **2** appear to be made up of a single polymeric helical backbone rather than numerous short oligomeric helices, creating aquapores with a narrow cavity of ~ 2.8 Å across for transporting water molecules across the lipid bilayer membranes.[11c]

These recently reported water-containing crystals of $\mathbf{2}\bullet 2H_2O$ were grown via slow evaporation of **2**-containing anhydrous CH_2Cl_2 at room temperature for weeks. Since commercially available anhydrous CH_2Cl_2 typically contains no more than 0.001% water by weight, a molar ratio of CH_2Cl_2 over water molecules under the crystal growth conditions can be calculated to be 5304 on the basis of their respective molecular weights of 84.93 and 18.02 g/mol. This points to an exceptional selectivity factor of at least 5304 in recognizing water over CH_2Cl_2 molecules by the aquapore contained in $(\mathbf{2})_n$.

A few of other intriguing questions we attempt to answer in this work concern the ability of the aquapore contained in the helical stack of $(\mathbf{2})_n$ to accommodate other non-water molecules and the binding selectivity among the molecules that can be recognized by the aquapore. In this regard, a slow diffusion of an equal volume (1 mL) of either acetone, ethyl acetate, acetone or methanol into **1**-containing CH_2Cl_2 solution produces either no or crystals of **2**•MeOH containing regularly arrayed chains of MeOH molecules in the hollow tubular cavity of $(\mathbf{2})_n$, suggesting that a recognition of either water or MeOH molecules by the aquapore in $(\mathbf{2})_n$ proceeds in a selective manner.

Organic & Biomolecular Chemistry Accepted Manuscript

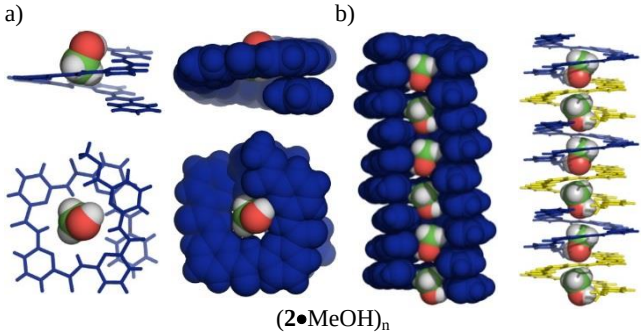

Fig. 2 (a) illustrates a helically folded pentameric backbone in **2** that is rigidified by an intramolecular H-bonding network and able to bind to one methanol molecule, and (b) shows 1D helical packing involving numerous molecules of **2** via aromatic π-π stacking forces assisted by the complementary "sticky" end groups that forms H-bonds of 2.41 and 3.01 Å. From CPK model of (**2**●MeOH)$_n$ shown in (b), a discrete chain of MeOH molecules is trapped inside the hollow cavity, and no direct contacts among MeOH molecules can be seen.

Structural analysis of **2**●MeOH reveals an expected existence of a strong intramolecular H-bonding network that restricts the conformational freedom of the amide bonds in **2** and induces its aromatic backbone to curve in one direction, and eventually into a helical conformation (Fig. 2a). Similarly, the end ester and phenyl groups (Fig. 1b) designed to be complementary and "sticky" do stick to each other to form one moderate H-bond of 2.405 Å and one very weak H-bond of 3.018 Å between the ester carbonyl O-atom and phenyl aromatic protons. These numerous weak but attractive H-bonding forces work together with aromatic π-π stacking forces to enable numerous short helices to efficiently pack on top of each other to produce an enclosed hollow cavity of about 2.75 Å in diameter, which allows small MeOH molecules to sit inside the cavity interior via stabilizing strong H-bonds of 2.094 and 2.352 Å and many other weak H-bonds and van der Waals interactions between the host and guest molecules (Fig 2b). Computationally by using Dreiding force field[12a] for calculating aromatic π−π stacking forces and the first principle calculation at the B3LYP/6-311G(2d,p) level for H-bonds formed by "sticky" ends and MeOH stabilization by the host, it was found that efficient full overlap of helical backbones of **2** via aromatic π−π stacking provides the major driving force, contributing 32.04 kcal/mol per molecule of **2** to the formation of 1D helical stack. This full overlap is made possible as a result of the two feeble yet indispensable intermolecular H-bonds of 1.96 kcal/mol in strength arising from the two "sticky" ends. Every host molecule of **2** provides additional average stabilization energy of 9.11kcal/mol per MeOH molecule.

From the above analyses, it can be seen that the aquapores in (**2**)$_n$ selectively recognize water and MeOH molecules over other small molecules including CH_2Cl_2, acetone, ethyl acetate, acetone,etc. To further discern the selectivity between water and MeOH molecules, we designed a series of crystallization experiments involving growing crystals of **2**●2H_2O via slow diffusion of a certain volume of mixed solvents containing MeOH and H_2O in varying ratios into 1 mL CH_2Cl_2 that contains 1 mg of **2** in a tightly capped vial over 10-15 days at room temperature (Table 1). Crystallographic analyses of all the crystals grown under the conditions tested demonstrate an

Table 1. Crystal growth conditions for **2**●2H_2O and **2**$_n$●2H_2O (n = 1-4) at varying ratios of MeOH/H_2O (v:v) at room temperature.

	2	CH_2Cl_2	H_2O	MeOH	Crystal growth time
2●2H_2O			0 µl	0 µl	
2$_1$●2H_2O				10 µl	
2$_2$●2H_2O	1 mg	1 mL	20 µl	100 µl	10-15 days
2$_3$●2H_2O				200 µl	
2$_4$●2H_2O				800 µl	

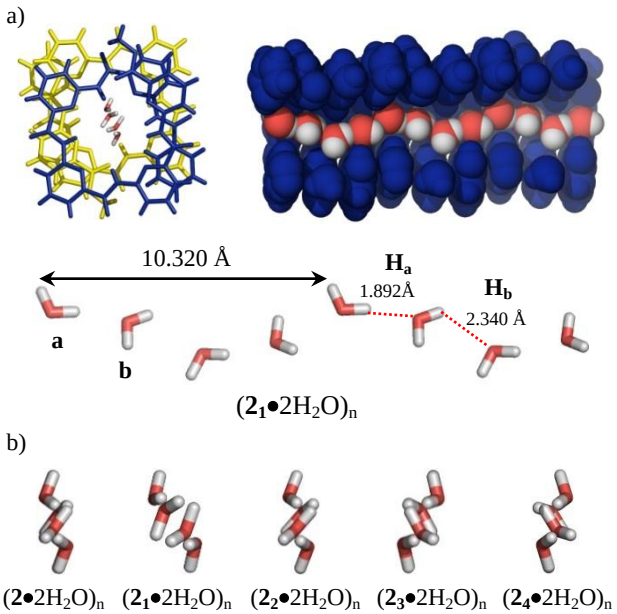

Fig. 3 Schematic illustrations of 1D water chains taken from the crystal structure of **2**●2H_2O and **2**$_n$●2H_2O (n = 1-4). As shown in (b), every water chain in **2**$_n$●2H_2O (n = 1-4) also contains two types of water molecules, **a** and **b** as well as two types of the intermolecular H-bonds, **H**$_a$ and **H**$_b$.

invariable trapping of only water molecules, not MeOH molecules, inside the aquapores formed by molecules of **2**. On the basis of the smallest volumetric ratio of 20 µl:800 µl for water:MeOH that corresponds to a water:MeOH molar ratio of 1:17.7, a selectivity factor of 17.7 can be estimated. Further considering that the aquapores are exclusively occupied by water molecules, the actual selectivity could be much higher than 17.7 by many orders of magnitude.

Remarkably similar to the structure of **2**●2H_2O, all the crystal structures from **2**$_1$●2H_2O to **2**$_4$●2H_2O contain a helically folded structure of **2** that stacks on top of each other to produce 1D hollow cavity, which subsequently trapped a helically arrayed H-bonded 1D water chain with four water molecules per helical turn (Fig. 3a). From the top views of the water chains presented in Fig. 3b, the helically arranged water chains in (**2**●2H_2O)$_n$, (**2**$_1$●2H_2O)$_n$ and (**2**$_2$●2H_2O)$_n$ might have a helical handedness different from those found in (**2**$_3$●2H_2O)$_n$ and (**2**$_4$●2H_2O)$_n$. A significant alteration in topology also exists for the water chains

Organic & Biomolecular Chemistry Accepted Manuscript

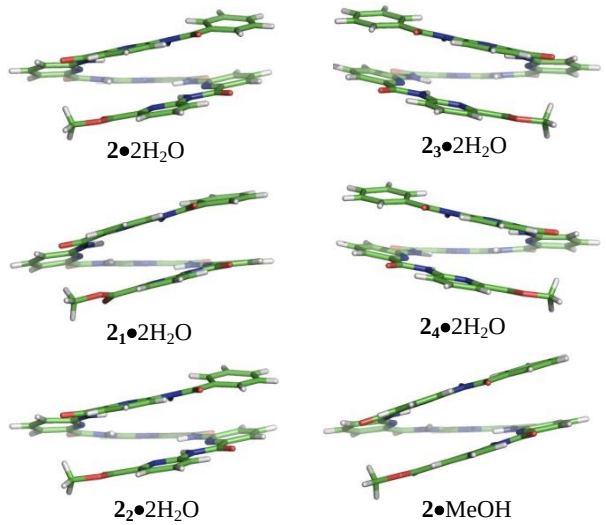

Fig. 4 Side views of the helically folded aromatic backbone of **2** in the crystal structures of **2**•$2H_2O$, $\mathbf{2_1}$•$2H_2O$, $\mathbf{2_2}$•$2H_2O$, $\mathbf{2_3}$•$2H_2O$, $\mathbf{2_4}$•$2H_2O$ and **2**•MeOH. Note that molecules of **2** from $\mathbf{2_3}$•$2H_2O$ and $\mathbf{2_4}$•$2H_2O$ might have a helical handedness different from others; this, however, cannot be unambiguously confirmed.

found in (**2**•$2H_2O$)$_n$, ($\mathbf{2_1}$•$2H_2O$)$_n$ and ($\mathbf{2_3}$•$2H_2O$)$_n$, but those from (**2**•$2H_2O$)$_n$, ($\mathbf{2_2}$•$2H_2O$)$_n$ and ($\mathbf{2_4}$•$2H_2O$)$_n$ are topologically more akin to each other if their helical handedness is not considered.

These structures additionally differ from each other in many subtle ways on how the short helices interact with each other and with the trapped water molecules as well as how the water molecules associate with each other to form the water chains. Specifically, (1) the helical pitch, which dictates the intermolecular distance between the two water molecules with an identical orientation from the 1D water chain, ranges from 10.320 Å in ($\mathbf{2_1}$•$2H_2O$)$_n$ to 10.416 Å in (**2**•$2H_2O$)$_n$, (2) the average aromatic π-π stacking distance ranges from 3.440 to 3.472 Å, (3) some structural changes in the helical backbone (Fig 4) and around the 'sticky ends" are observed, (4) the two intermolecular H-bonds H_a and H_b (Fig 3a) fall within 1.841-1.901 Å and 2.264-2.395 Å, respectively, and (5) the two weak intermolecular H-bonds H_1 and H_2 formed by the two "sticky" ends vary from 2.746-2.799 Å & 2.821-3.045 Å (Table 2) , respectively. In terms of percent variation, intermolecular H-bonds seem to undergo the largest changes in response to the external stimulus, e.g., methanol in our current study.

Energetically, these water chain-containing aquapores would differ in strength of the H-bonds arising from the "sticky" ends ($\mathbf{E_{SE}}$), aromatic π-π stacking interaction ($\mathbf{E_{\pi}}$), stabilization of two types of water molecules **a** and **b** (Fig. 3) with different orientations by the hosts ($\mathbf{E_{HG}} = \mathbf{E_{HGa}} + \mathbf{E_{HGb}}$), and the two types of H-bond $\mathbf{H_a}$ and $\mathbf{H_b}$ (Fig. 3) contained in the water chains ($\mathbf{E_H} = \mathbf{E_{Ha}} + \mathbf{E_{Hb}}$). Therefore, single point energy calculations on the corresponding structural motifs directly taken out from their respective crystal structures were carried out by using Dreiding force field[12a] for aromatic π-π stacking energy $\mathbf{E_{\pi}}$ and the first principle calculation at the B3LYP/6-311G(2d,p) level for all the other three energy components (Table 3). Our computations show that variations in varying energy components among all the

Table 2. H-bonds formed by the two "sticky" ends from the crystal structures of **2**•$2H_2O$, $\mathbf{2_1}$•$2H_2O$, $\mathbf{2_2}$•$2H_2O$, $\mathbf{2_3}$•$2H_2O$, $\mathbf{2_4}$•$2H_2O$ and **2**•MeOH.

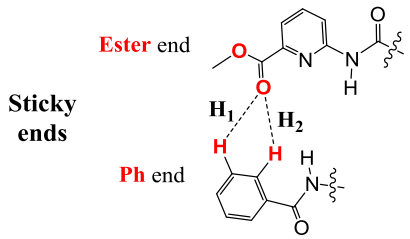

	2•$2H_2O$	$\mathbf{2_1}$•$2H_2O$	$\mathbf{2_2}$•$2H_2O$	$\mathbf{2_3}$•$2H_2O$	$\mathbf{2_4}$•$2H_2O$	**2**•MeOH
$\mathbf{H_1}$	2.821 Å	3.045 Å	2.848 Å	2.940 Å	2.876Å	2.405 Å
$\mathbf{H_2}$	2.746 Å	2.799 Å	2.758 Å	2.771 Å	2.754 Å	3.018 Å

structures are apparent with the largest variations of 28.6% and 11.5% arising from aromatic π-π stacking ($\mathbf{E_{\pi}}$) and host-guest ($\mathbf{E_{HG}}$) interactions, respectively. Although the energetic variation in total H-bond strength is much smaller (7.3%), which provide attractive forces to stabilize both the full overlap of helically folded aromatic backbones ($\mathbf{E_{SE}}$) and the 1D water chains remain ($\mathbf{E_H}$), both of its two components $\mathbf{E_{Ha}}$ and $\mathbf{E_{Ha}}$ have very large variations of 18.3% and 22.3%, respectively. These data suggest that both the water chain and aquapores assembled from aquafoldamer molecules are very dynamic in structure and particularly in energy, and that the external stimuli such as presence of excessive amounts of methanol during the crystal growth exert the largest impact on aromatic π-π stacking and a very substantial influence on both the intermolecular H-bonds in the 1D water chains and the host-guest interactions, while the H-bonds from the "sticky" ends remain much less affected. Further, it might be of an additional interest to note that the water chain-containing aquapores, with their total energy, $\mathbf{E_{Total}}$, ranging from 59.29 ($\mathbf{2_2}$•$2H_2O$, Table 3) to 62.55 kcal/mol (**2**•$2H_2O$, Table 3), seem to be robust enough to withstand methanol present in solution in a 19-fold excess in volume with respective to water, but a 39-fold excess of methanol likely produces a dramatic impact on the aquapore structure, leading to an abrupt decrease in its energy and stability with an $\mathbf{E_{Total}}$ value of 54.66 kcal/mol.

Even more dramatic dynamics around the region involving "sticky ends" in the assembled aquapores can also be seen by comparing the crystal structure containing aligned methanol molecules **2**•MeOH with any other crystal structure containing 1D water chains such as $\mathbf{2_1}$•$2H_2O$ (Table 2 and Fig. 5). Each "sticky end" contains two types of H-bonds, $\mathbf{H_1}$ and $\mathbf{H_2}$, and the two H-bonds from **2**•MeOH are either the shortest (2.405 Å) among $\mathbf{H_1}$ type or longest (3.018Å) among $\mathbf{H_2}$ type. More importantly, $\mathbf{H_1}$ type H-bond is shorter than $\mathbf{H_2}$ type H-bond in **2**•MeOH, and this relative magnitude is reversed in all the water-containing structures including $\mathbf{2_1}$•$2H_2O$ with $\mathbf{H_2}$ type H-bond (2.799 Å, Fig. 5) being shorter that $\mathbf{H_1}$ type (3.045 Å, Fig. 5). This suggests a significant re-arrangement of the "sticky end" in order for the same host **2** to accommodate water rather than methanol molecules in the assembled hollow cavity. By

Organic & Biomolecular Chemistry Accepted Manuscript

Table 3. Computationally determined energetic profiles[a] in kcal/mol associated with the structures of **2**●$2H_2O$ and $\mathbf{2_n}$●$2H_2O$ (n = 1-4).

Water complexes	E_{SE}	E_{π}	E_{HG}			E_H			E_{Total} ($E_{SE} + E_{\pi} + E_{HG} + E_H$)
			E_{HGa}	E_{HGb}	E_{Total}	E_{Ha}	E_{Hb}	E_{Total}	
2●$2H_2O$	2.28	31.09	9.14	12.29	21.43	4.15	3.60	7.75	62.55
$\mathbf{2_1}$●$2H_2O$	2.39	28.22	10.86	12.34	23.20	4.83	3.53	8.36	62.17
$\mathbf{2_2}$●$2H_2O$	2.24	26.08	9.98	12.78	22.76	5.08	3.13	8.21	59.29
$\mathbf{2_3}$●$2H_2O$	2.43	28.65	10.06	11.57	21.63	4.31	4.03	8.34	61.05
$\mathbf{2_4}$●$2H_2O$	2.31	22.20	9.96	12.05	22.01	4.29	3.85	8.14	54.66
Variation%	7.8%	**28.6%**	15.8%	9.5%	11.5%	18.3%	22.3%	7.3%	12.6%

[a] Every energy profile calculated include the H-bonds arising from the "sticky" ends (E_{SE}), aromatic π-π stacking interaction (E_{π}), stabilization of water molecules **a** and **b** (Fig. 3) by the hosts (E_{HG}), and the two types of H-bonds H_a and H_b (Fig. 3) contained in the water chains (E_H). The values for variation% were obtained by dividing the difference between the largest and smallest numbers using the largest number within the same category.

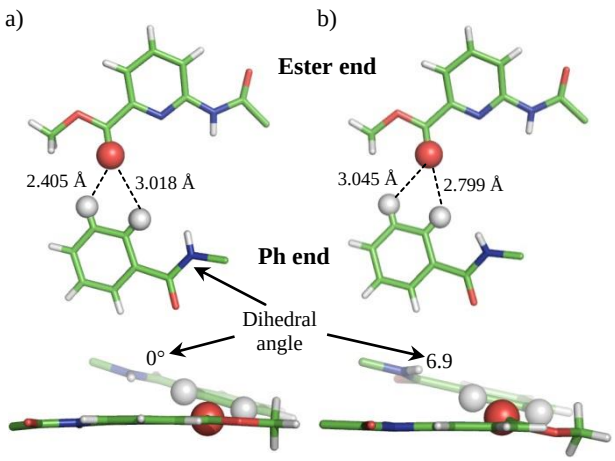

E_{SE} = 1.96 kcal/mol
2●MeOH

E_{SE} = 2.36 kcal/mol
$\mathbf{2_1}$●$2H_2O$

Fig. 5 Top and side views of the "sticky" ends in (a) **2**●MeOH and (b) $\mathbf{2_1}$●$2H_2O$, which demonstrate significant differences around the "sticky" ends found in **2**●MeOH and $\mathbf{2_1}$●$2H_2O$ in order to accommodate MeOH and water molecules in their interiors. The "sticky" ends from other water-containing structures such as **2**●$2H_2O$, $\mathbf{2_2}$●$2H_2O$, $\mathbf{2_3}$●$2H_2O$ and $\mathbf{2_4}$●$2H_2O$ have a near-identical look. Also see Fig. 4 for other differences in the helical backbone of **2** among $\mathbf{2_n}$●$2H_2O$ (n=1-4).

comparing the H-bond length of $\mathbf{H_1}$ and $\mathbf{H_2}$ types in **2**●MeOH respectively with those of $\mathbf{H_2}$ and $\mathbf{H_1}$ types in $\mathbf{2_1}$●$2H_2O$ (Fig. 5), the H-bonds in **2**●MeOH are apparently shorter in overall. Surprisingly, the overall strength involving the two H-bonds in **2**●MeOH with a computationally determined value of 1.96 kcal/mol is energetically less stable than that found in $\mathbf{2_1}$●$2H_2O$ by 0.40 kcal/mol (Fig. 5). A careful comparison of the side views of the "sticky end' regions in **2**●MeOH and $\mathbf{2_1}$●$2H_2O$ reveals a very minor difference in planarity involving the three H-bond donor and acceptor atoms, i.e., one carbonyl O-atom from the ester end and two aromatic H-atoms from the Ph end. In more details, the carbonyl O-atom from the ester end of **2**●MeOH stays coplanar with the ester end, and therefor deviates from the aromatic plane of the Ph end that contains the two H-atoms more than the corresponding O-atom from $\mathbf{2_1}$●$2H_2O$ whose carbonyl O-atom slightly points away from the plane defined by the ester end and toward the two H-atoms. This seemingly more planar arrangement involving the three H-bond donor and acceptor atoms in $\mathbf{2_1}$●$2H_2O$ likely enhances the orbital overlapping extent among the donor and acceptor atoms, and increases the overall strength of the two H-bonds. A significant re-arrangement is additionally seen in the helically shaped aromatic backbone of **2** with parts of its helical backbone being comparatively more flat in **2**●MeOH than the corresponding parts in all the water-containing structures (Fig. 4).

Experimental section

Pentamer **2** was synthesized using previously established procedures +reported by us.[11c] All solvents were of reagent grade quality and used as supplied by the manufacturers.

Crystallization Experiments. X-ray quality crystals of **2**●MeOH was grown via slow diffusion of 0.9 mL MeOH into 0.6 mL dichloromethan containing 2 mg of **2** in a capped vial over 15 days at room temperature. And X-ray quality crystals of $\mathbf{2_n}$●$2H_2O$ (n = 1-4) were grown via slow diffusion of a certain volume of MeOH/H_2O at varying ratios into 1 mL of dichloromethane containing 1 mg of **2** in a capped vial over 10-15 days at room temperature.

First principle Computations. All the calculations except for the energy of aromatic π-π interactions were carried out on the structural motifs taken from the respective crystal structures by utilizing the either the Gaussian 03[12b] or Gaussian 09[12c] program package. The Becke's three parameter hybrid functional with the Lee-Yang-Parr correlation functional (B3LYP)[12d] method was employed to do the calculations. Unless otherwise stated, the 6-311+G(2d, p)[12e] basic from the Gaussian basis set library has been used in all the single point energy calculations.

Computations by Dreiding Force Field.[12a] The dreiding force field was used to calculate the energy of aromatic π-π interactions as tabulated in Table 3 with the corresponding structural motifs taken from the respective crystal structures. The convergence tolerance is $2X10^{-5}$ kcal/mol for the energy, 0.001 kcal/mol/A for

Organic & Biomolecular Chemistry Accepted Manuscript

the force, 0.001 GPa for the stress and 10^{-5} A for the displacement. The Ewald method is used for calculating the electrostatic and the van der Waals terms. The accuracy is 10^{-5} kcal/mol. The repulsive cutoff is 6 Å for the van der Waals term. For the hydrogen bond term, the summation method is atom based and the truncation method is cubic spline with cutoff distance of 4.5 Å.

X-ray Crystallography. X-ray single crystal data were collected on a Bruker APEX diffractometer with a CCD detector and graphite-monochromated MoKα radiation using a sealed tube (2.4 kW) at 223(2) K. Absorption corrections were made with the program SADABS[13a] and the crystallographic package SHELXTL[13b] was used for all calculations. CCDC numbers for **2**•MeOH, $\mathbf{2_1}$•$2H_2O$, $\mathbf{2_2}$•$2H_2O$, $\mathbf{2_3}$•$2H_2O$, and $\mathbf{2_4}$•$2H_2O$ are 1419114, 1419115, 1419116, 1419117 and 1419118, respectively.

Conclusions

Although the hollow cavity in $(\mathbf{1})_n$ selectively recognizes guest molecules decreasing in the order of MeOH > H_2O > CH_2Cl_2, a similar hollow cavity in $(\mathbf{2})_n$ created from the structurally similar molecules of **2** does not recognize CH_2Cl_2 at all, and displays a much higher affinity toward H_2O than MeOH molecules. Contrary to the formation of a continuous H-bonded water chain in $(\mathbf{2}\bullet 2H_2O)_n$, methanol molecules are trapped inside the hollow cavity in $(\mathbf{2}\bullet MeOH)_n$ in a discrete fashion. By doping 10 to 800 µl of methanol into crystallization conditions containing 20 µl of water, both the structural dynamic and energy profile of water chain-containing aquapores formed from **2** under different conditions have been further studied. While the overall structures involving the water chains and aquapores remain stable and similar, these water chain-containing structures do undergo dynamic re-arrangements in response to varying amounts of methanol molecules and differ subtly in many aspects including the helical pitch, the average aromatic π-π stacking distance/strength, and the length/strength of the H-bonds responsible for inducing helical stacks and stabilizing 1D water chains. Energetically, the external stimuli seem to exert its substantial impacts on the various structural motifs with an increasing order of the H-bonds from the "sticky" ends < the H-bonds in the 1D water chains or the host-guest interactions < the aromatic π-π stacking. Lastly, the one-dimensionally assembled aquapores dynamically undergo a significant re-arrangement in both the "sticky end" region and helically shaped aromatic backbone in order to accommodate water, rather than methanol, molecules in their hollow cavities.

Financial supports by the Institute of Bioengineering and Nanotechnology (Biomedical Research Council, Agency for Science, Technology and Research, Singapore), the A*STAR Computational Resource Centre through the use of its high performance computing facilities and National Natural Science Foundation of China (21172047 to Y.H.)

Notes and references

[a] *Faculty of Chemical Engineering and Light Industry, Guang Dong University of Technology, Guang Dong, 510006, China*

[b] *School of Chemical and Environmental Engineering, Wuyi University 99 Yingbin Road, Jiangmen, Guangdong, 529020, China*

[c] *Institute of Bioengineering and Nanotechnology, 31 Biopolis Way, The Nanos, Singapore 138669. E-mail: hqzeng@ibn.a-star.edu.sg; Tel: (+) 65-6824-7115*

1. (a) K. Murata, K. Mitsuoka, T. Hirai, T. Walz, P. Agre, J. B. Heymann, A. Engel and Y. Fujiyoshi, *Nature*, 2000, **407**, 599; (b) E. Tajkhorshid, P. Nollert, M. Ø. Jensen, L. J. W. Miercke, J. O'Connell, R. M. Stroud and K. Schulten, *Science.*, 2002, **296**, 525.
2. M. Barboiu and A. Gilles, *Acc. Chem. Res.*, 2013, **46**, 2814.
3. (a) B. Henrik, S. Dieter and P. Philip, *Angew. Chem, Int. Ed.*, 2002, **41**, 754; (b) L. E. Cheruzel, M. S. Pometun, M. R. Cecil, M. S. Mashuta, R. J. Wittebort and R. M. Buchanan, *Angew. Chem, Int. Ed.*, 2003, **42**, 5452; (c) P. S. Sidhu, K. A. Udachin and J. A. Ripmeester, *Chem. Commun.*, 2004, 1358; (d) B. K. Saha and A. Nangia, *Chem. Commun.*, 2005, 3024; (e) K. Ono, K. Tsukamoto, R. Hosokawa, M. Kato, M. Suganuma, M. Tomura, K. Sako, K. Taga and K. Saito, *Nano Lett.*, 2009, **9**, 122; (f) Y. L. Duc, M. Michau, A. Gilles, V. Gence, Y.-M. Legrand, A. Lee, S. Tingry and M. Barboiu, *Angew. Chem., Int. Ed.*, 2011, **50**, 11366.
4. (a) U. S. Raghavender, S. Aravinda, N. Shamala, Kantharaju, R. Rai and P. Balaram, *J. Am. Chem. Soc.*, 2009, **131**, 15130; (b) U. S. Raghavender, Kantharaju, S. Aravinda, N. Shamala and P. Balaram, *J. Am. Chem. Soc.*, 2010, **132**, 1075; (c) R. Natarajan, J. P. H. Charmant, A. G. Orpen and A. P. Davis, *Angew. Chem,, Int. Ed.*, 2010, **49**, 5125.
5. (a) M. S. Kaucher, M. Peterca, A. E. Dulcey, A. J. Kim, S. A. Vinogradov, D. A. Hammer, P. A. Heiney and V. Percec, *J. Am. Chem. Soc.*, 2007, **129**, 11698; (b) C. B. Hu, Z. X. Chen, G. F. Tang, J. L. Hou and Z. T. Li, *J. Am. Chem. Soc*, 2012, **134**, 8384; (c) X. B. Zhou, G. D. Liu, K. Yamato, Y. Shen, R. X. Cheng, X. X. Wei, W. L. Bai, Y. Gao, H. Li, Y. Liu, F. T. Liu, D. M. Czajkowsky, J. F. Wang, M. J. Dabney, Z. H. Cai, J. Hu, F. V. Bright, L. He, X. C. Zeng, Z. F. Shao and B. Gong, *Nat. Comm.*, 2012, **3**, 949.
6. (a) A. J. Kim, M. S. Kaucher, K. P. Davis, M. Peterca, M. R. Imam, N. A. Christian, D. H. Levine, F. S. Bates, V. Percec and D. A. Hammer, *Adv. Funct. Mat.*, 2009, **19**, 2930; (b) W. Si, L. Chen, X. B. Hu, G. F. Tang, Z. X. Chen, J. L. Hou and Z. T. Li, *Angew. Chem,, Int. Ed.*, 2011, **50**, 12564.
7. For some selected reviews in foldamers, see: (a) S. H. Gellman, *Acc. Chem. Res.*, 1998, **31**, 173; (b) D. J. Hill, M. J. Mio, R. B. Prince, T. S. Hughes and J. S. Moore, *Chem. Rev.*, 2001, **101**, 3893; (c) R. P. Cheng, S. H. Gellman and W. F. DeGrado, *Chem. Rev.*, 2001, **101**, 3219; (d) M. S. Cubberley and B. L. Iverson, *Curr. Opin. Chem. Biol.*, 2001, **5**, 650; (e) A. R. Sanford and B. Gong, *Curr. Org. Chem.*, 2003, **7**, 1649; (f) R. P. Cheng, *Curr. Opin. Struc. Biol.*, 2004, **14**, 512; (g) B. Gong, *Acc. Chem. Res.*, 2008, **41**, 1376; (h) Z. T. Li, J. L. Hou and C. Li, *Acc. Chem. Res.*, 2008, **41**, 1343; (i) W. S. Horne and S. H. Gellman, *Acc. Chem. Res.*, 2008, **41**, 1399; (j) I. Saraogi and A. D. Hamilton, *Chem. Soc. Rev.*, 2009, **38**, 1726; (k) G. Guichard and I. Huc, *Chem. Commun.*, 2011, **47**, 5933; (l) B. Baptiste, F. Godde and I. Huc, *ChemBioChem*, 2009, **10**, 1765; (m) K. Yamato, M. Kline and B. Gong, *Chem. Commun.*, 2012, **48**, 12142; (n) D.-W. Zhang, X. Zhao, J.-L. Hou and Z.-T. Li, *Chem. Rev.*, 2012, **112**, 5271; (o) W. Q. Ong and H. Q. Zeng, *J. Incl. Phenom. Macrocycl. Chem.*, 2013, **76**, 1; (p) H. L. Fu, Y. Liu and H. Q. Zeng, *Chem. Commun.*, 2013, **49**, 4127.
8. For folding molecules derived from methoxybenzene, pyridone and fluorobenzene build blocks recently reported by us, see: (a) B. Qin, C. Sun, Y. Liu, J. Shen, R. J. Ye, J. Zhu, X.-F. Duan and H. Q. Zeng, *Org. Lett.*, 2011, **13**, 2270; (b) Y. Yan, B. Qin, Y. Y. Shu, X.

Organic & Biomolecular Chemistry Accepted Manuscript

Y. Chen, Y. K. Yip, D. W. Zhang, H. B. Su and H. Q. Zeng, *Org. Lett.*, 2009, **11**, 1201; (c) Y. Yan, B. Qin, C. L. Ren, X. Y. Chen, Y. K. Yip, R. J. Ye, D. W. Zhang, H. B. Su and H. Q. Zeng, *J. Am. Chem. Soc.*, 2010, **132**, 5869; (d) Z. Y. Du, C. L. Ren, R. J. Ye, J. Shen, Y. J. Lu, J. Wang and H. Q. Zeng, *Chem. Commun.*, 2011, **47**, 12488; (e) C. L. Ren, V. Maurizot, H. Q. Zhao, J. Shen, F. Zhou, W. Q. Ong, Z. Y. Du, K. Zhang, H. B. Su and H. Q. Zeng, *J. Am. Chem. Soc.*, 2011, **133**, 13930; (f) C. L. Ren, F. Zhou, B. Qin, R. J. Ye, S. Shen, H. B. Su and H. Q. Zeng, *Angew. Chem., Int. Ed.*, 2011, **50**, 10612; (g) C. L. Ren, S. Y. Xu, J. Xu, H. Y. Chen and H. Q. Zeng, *Org. Lett.*, 2011, **13**, 3840.

9. For various functions elaborated on the folding molecules over the recent years by us, see: (a) B. Qin, C. L. Ren, R. J. Ye, C. Sun, K. Chiad, X. Y. Chen, Z. Li, F. Xue, H. B. Su, G. A. Chass and H. Q. Zeng, *J. Am. Chem. Soc.*, 2010, **132**, 9564; (b) J. Shen, W. L. Ma, L. Yu, J.-B. Li, H.-C. Tao, K. Zhang and H. Q. Zeng, *Chem. Commun.*, 2014, **50**, 12730; (c) W. Q. Ong, H. Q. Zhao, C. Sun, J. E. Wu, Z. C. Wong, S. F. Y. Li, Y. H. Hong and H. Q. Zeng, *Chem. Commun.*, 2012, **48**, 6343; (d) C. Sun, C. L. Ren, Y. C. Wei, B. Qin and H. Q. Zeng, *Chem. Commun.*, 2013, **49**, 5307; (e) B. Qin, L. Y. Jiang, S. Shen, C. Sun, W. X. Yuan, S. F. Y. Li and H. Q. Zeng, *Org. Lett.*, 2011, **13**, 6212; (f) Z. Y. Du, B. Qin, C. Sun, Y. Liu, X. Zheng, K. Zhang, A. H. Conney and H. Q. Zeng, *Org. Biomol. Chem.*, 2012, **10**, 4164; (g) H. Q. Zhao, J. Shen, J. J. Guo, R. J. Ye and H. Q. Zeng, *Chem. Commun.*, 2013, **49**, 2323.

10. (a) W. Q. Ong, H. Q. Zhao, Z. Y. Du, J. Z. Y. Yeh, C. L. Ren, L. Z. W. Tan, K. Zhang and H. Q. Zeng, *Chem. Commun.*, 2011, **47**, 6416; (b) H. Q. Zhao, W. Q. Ong, X. Fang, F. Zhou, M. N. Hii, S. F. Y. Li, H. B. Su and H. Q. Zeng, *Org. Biomol. Chem.*, 2012, **10**, 1172; (c) W. Q. Ong, H. Q. Zhao, X. Fang, S. Woen, F. Zhou, W. L. Yap, H. B. Su, S. F. Y. Li and H. Q. Zeng, *Org. Lett.*, 2011, **13**, 3194.

11. (a) H. Q. Zhao, W. Q. Ong, F. Zhou, X. Fang, X. Y. Chen, S. F. Y. Li, H. B. Su, N.-J. Cho and H. Q. Zeng, *Chem. Sci.*, 2012, **3**, 2042; (b) F. Zhou, H. L. Fu, W. Q. Ong, R. J. Ye, W. X. Yuan, Y.-J. Lu, Y.-P. Huo, K. Zhang, H. B. Su and H. Q. Zeng, *Org. Biomol. Chem.*, 2012, **10**, 5525; (c) H. Q. Zhao, S. Sheng, Y. H. Hong and H. Q. Zeng, *J. Am. Chem. Soc.*, 2014, **136**, 14270.

12. (a) S. L. Mayo, B. D. Olafson and W. A. Goddard III, *J. Phys. Chem.*, 1990, **94**, 8897; (b) M. J. Frisch, in *Gaussian 03, Gaussian, Inc.*, Wallingford CT,, 2004; (c) M. J. Frisch, in *Gaussian 09, Gaussian, Inc.*, Wallingford CT,, 2009; (d) A. D. Becke, *J. Chem. Phys.*, 1993, **98**, 5648; (e) G. A. Petersson, A. Bennett, T. G. Tensfeldt, M. A. Al-Laham, W. A. Shirley and J. Mantzaris, *J. Chem. Phys.*, 1988, **89**, 2193.

13. (a) Sheldrick, G. M., *SADABS, Software for Empirical Absorption Corrections*, University of Göttingen (Germany),, 2000; (b) *SHELXTL, Reference Manual*, version 5.1, Bruker AXS, Analytical X-Ray Systems, Madison, WI, USA,, 1997.

Organic & Biomolecular Chemistry Accepted Manuscript